Role of Interactions in ^{87}Rb-^{40}K Bose-Fermi Mixtures in a 3D Optical Lattice

Th. Best, S. Will, U. Schneider, L. Hackermüller, D. van Oosten,* and I. Bloch

Institut für Physik, Johannes Gutenberg-Universität Mainz, Staudinger Weg 7, 55128 Mainz, Germany

D.-S. Lühmann

I. Institut für Theoretische Physik, Universität Hamburg, Jungiusstr. 9, 20355 Hamburg, Germany
(Received 22 July 2008; published 23 January 2009)

We investigate the effect of interspecies interaction on a degenerate mixture of bosonic ^{87}Rb and fermionic ^{40}K atoms in a three-dimensional optical lattice potential. Using a Feshbach resonance, the ^{87}Rb-^{40}K interaction is tuned over a wide range. Through an analysis of the ^{87}Rb momentum distribution, we find a pronounced asymmetry between strong repulsion and strong attraction. In the latter case, we observe a marked shift in the superfluid to Mott insulator transition, which we attribute to a renormalization of the Bose-Hubbard parameters due to self-trapping.

Mixtures of quantum gases in optical lattices form novel quantum many-body systems, whose properties are governed by the interplay of quantum statistics, inter- and intraspecies interactions, as well as the relative number of atoms of the components. In particular, degenerate Bose-Fermi mixtures, which rarely occur in nature and have only recently come within experimental reach, have stimulated theoretical investigations. Already for the simplest description of such an interacting mixture in terms of a single-band Bose-Fermi Hubbard model, a variety of quantum phases have been predicted [1–3], including charge-density waves, polaronlike quasiparticles [4], as well as perturbed Mott-insulating (MI) states [5,6]. The correlated (or anticorrelated) movement of composite particles can result in exotic superfluids [7]. Moreover, within a limited parameter regime, supersolid behavior has been predicted [8,9]. Unlike in the pure bosonic case, realistic descriptions of the mixture need to consider multiband physics [10], finite-temperature [11], physical loss channels, and the inhomogeneity present in optical lattice experiments. Recently, mixtures of bosonic ^{87}Rb and fermionic ^{40}K atoms in 3D optical lattices have been investigated at fixed attractive background scattering length in two independent experiments [12,13]. The authors found a shift of the visibility loss of the ^{87}Rb interference pattern towards shallower lattices, which has been interpreted as a shift of the bosonic superfluid to MI transition (see Ref. [14] for related work on a Bose-Bose mixture). Several mechanisms have been put forward to explain this shift; however, none could clearly be identified.

Here, we report on the realization of a quantum degenerate mixture of bosonic ^{87}Rb and fermionic ^{40}K atoms with tunable interspecies interaction in a 3D optical lattice. We investigate the coherence properties of the bosonic component in the presence of fermions over a wide range of interspecies interactions, from strongly attractive to strongly repulsive, for varying admixture of fermions. At large fermion fillings and attractive interspecies interactions, we find good agreement with a recent model of self-trapping [10]. This model predicts a significant renormalization of the Bose-Hubbard parameters, resulting in a shift of the superfluid to MI transition, in good agreement with our experimental results.

The starting point for our experiments is a degenerate mixture of 4×10^5 ^{87}Rb and up to 3×10^5 ^{40}K atoms in their respective hyperfine ground states $|F = 1, m_F = +1\rangle$ and $|F = \frac{9}{2}, m_F = -\frac{9}{2}\rangle$. The mixture is held in a crossed dipole trap, operated at a wavelength of 1030 nm. The ellipticity of the dipole beams makes the trap vertically tight enough to ensure interspecies overlap in the presence of gravitational sag.

A homogeneous magnetic field is applied in order to address the 2.9 G wide interspecies Feshbach resonance (FBR) at 546.9 G (parametrization taken from Ref. [15]). We can continuously tune the interspecies s-wave scattering length a_{bf} between $-170a_0$ and $+800a_0$ below the FBR, and between $-800a_0$ and $-200a_0$ above the FBR, with an accuracy of $\pm 10a_0$ close to the resonance, where a_0 is the Bohr radius. After 50 ms settling time for the magnetic field, a 3D optical lattice is adiabatically ramped up to a final depth in the range of $V_0 = 2$ to $17 E_r$ within 100 ms using an s-shaped ramp. The lattice wavelength $\lambda = 755$ nm is blue-detuned with respect to both ^{87}Rb and ^{40}K and chosen such that the lattice depths, as measured in units of the respective recoil energies $E_r = h^2/(2m_{b,f}\lambda^2)$, are equal for both species. This ensures maximum overlap of the Wannier functions, while the ratio of the tunneling rate of bosons and fermions is given by m_f/m_b. The blue lattice also causes an underlying harmonic anticonfinement which is (over-)compensated by the dipole trap [16].

After a hold time of 100 ms, which is long compared to the tunneling time for any lattice depth used, all traps as well as the magnetic field are instantaneously switched off,

and the atom clouds are allowed to expand during 18 ms
time of flight (TOF). The resulting interference pattern
of the ^{87}Rb atoms is recorded using standard absorption
imaging. From these images, we extract the contrast in
terms of the visibility [17]. Furthermore, we determine the
condensate fraction from a fit to the interference pattern.

By varying both the lattice depth and the magnetic field,
we probe the phases of the mixture. We have analyzed
scenarios with low ($N_f \approx 0.25N_b$), intermediate ($N_f \approx
0.5N_b$), and high ($N_f \approx 0.75N_b$) ^{40}K atom numbers.
Representative profiles of the visibility versus a_{bf} at high
N_f are shown in Fig. 1, for different values of the lattice
depth. For shallow lattices of less than $3E_r$, we find a high
visibility, which is almost independent of the interaction
strength. Also, for deeper lattices, at $a_{bf} \approx 0$, we recover a
monotonic decay of the visibility versus lattice depth com-
patible with the superfluid to MI transition in a pure ^{87}Rb
sample [17]. This demonstrates that the fermion cloud
becomes fully transparent for the bosons. For small abso-
lute values of a_{bf}, we observe a decrease of visibility
which is symmetrical around $a_{bf} = 0$ within our measure-
ment accuracy. The symmetry persists within the interval
$|U_{bf}| \lesssim U_{bb}$, where the interboson repulsion is strong
enough to effectively hinder bosonic double occupation
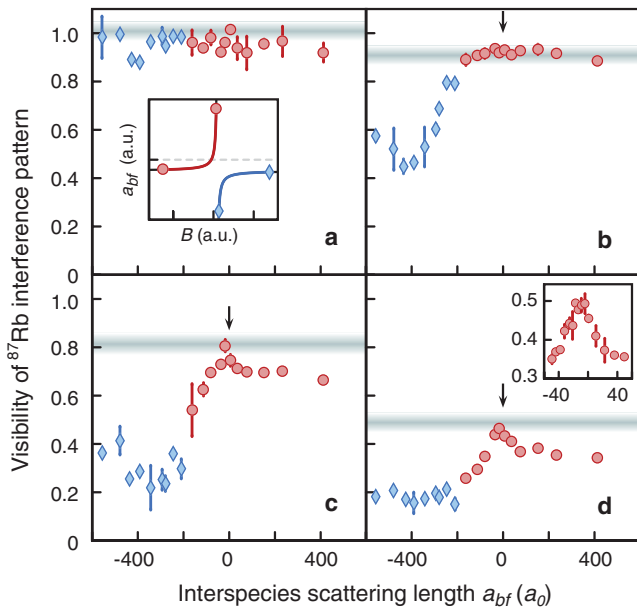of sites. Departing from this symmetry peak, we see a

FIG. 1 (color).   Profiles of visibility versus interspecies scatter-
ing length at lattice depths of (a) $3E_r$, (b) $5E_r$, (c) $9E_r$, and
(d) $12E_r$ for high N_f. At all lattice depths beyond $3E_r$, the
visibility shows a maximum at a position consistent with $a_{bf} =
0$ within the calibration uncertainty of $\pm 10a_0$ as indicated by the
arrow. The inset in part (d) shows a high-resolution scan taken at
$11E_r$. Blue diamonds (red circles) indicate points measured
above (below) resonance, as depicted in the inset in part (a).
The shaded regions represent the visibility measured for a pure
^{87}Rb cloud using the same experimental parameters.

further decay of visibility, which is significantly stronger
for intermediate attractive than for comparable repulsive
scattering lengths. This suggests a fundamental difference
in the underlying mechanisms on either side. The behavior
in the vicinity of the attractive background scattering
length as we observe it is similar to earlier measurements
[12,13]. Towards very strong attraction, we find a signifi-
cant loss of ^{87}Rb atoms, accompanied by an increase of
visibility. For strongly repulsive interactions, the visibility
remains almost constant on a high level. This indicates that
bosons and fermions do not occupy the same lattice sites in
this regime, consistent with phase separation in the lattice
[18], or the formation of a strongly anticorrelated mixed
phase [8,9,19]. Presently, we cannot distinguish between
both scenarios. For $a_{bf} > 400a_0$, we observe significant
atom losses; however, these are essentially independent of
the hold time, suggesting their occurrence early during
lattice loading, when the mixture is held just below the
FBR.

Based on the observations outlined above, we qualita-
tively identify five distinct regimes, i.e., lossless coexis-
tence in shallow lattices for all scattering lengths, and
regimes characterized by very strong interspecies attrac-
tion, intermediate attraction, weak interaction (of either
sign), and very strong repulsion for deeper lattices. This
classification also holds for low and intermediate values of
N_f, although the symmetric feature around $a_{bf} = 0$ is most
pronounced for the highest ^{40}K numbers.

We have verified that the visibility decrease is reversible
for interspecies scattering lengths in the range $-200a_0 \lesssim
a_{bf} \lesssim 400a_0$, when a_{bf} is tuned back to zero, provided that
the system is given enough time to re-equilibrate. This
suggests that the reduction of coherence is caused by a
reversible redistribution of the atomic densities during
the lattice loading. For attractive scattering lengths beyond
a critical value, we observe significant losses of ^{87}Rb
atoms, along with an increase in visibility. Despite this
increase, no condensate is discernible in the corresponding
TOF images. These findings are shown exemplarily in
Figs. 2(a) and 2(b). We fit two straight lines to the relevant
part of the visibility profiles and use their intersection point
as an estimate for the critical value. Figure 2(c) shows that
the resulting critical scattering lengths are independent of
N_f. This suggests that the visibility increase at strong
attractions is governed by the on-site physics. Recently,
the crucial role of the modification of Wannier orbitals due
to the mean-field on-site interaction in understanding the
attractively interacting mixture has been pointed out [10].
A strong interspecies attraction will not only enforce high
boson occupation numbers, but will also yield increased
on-site densities at given occupation due to admixture of
higher bands, which in turn could lead to a significant
increase in three-body loss rates.

We estimate this on-site density increase from a varia-
tional harmonic oscillator model, minimizing the total on-
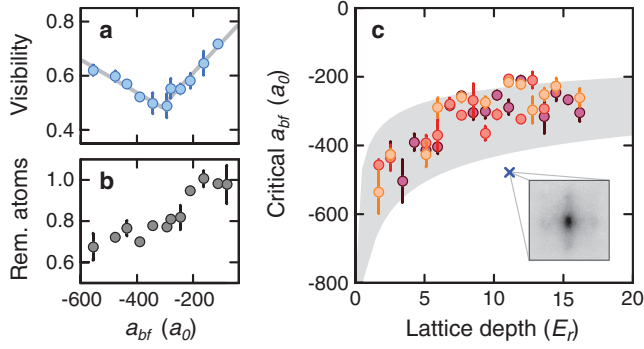site energy with respect to the width σ_b and σ_f of the

FIG. 2 (color). Onset of the loss-dominated regime. (a) Experimentally determined visibility minimum and (b) simultaneous ^{87}Rb loss feature at $V_0 = 9 E_r$ for intermediate N_f. (c) Critical a_{bf} determined from the visibility data, versus lattice depth for high, intermediate, and low N_f (darker colors for higher N_f). The shaded area gives an estimate of the scattering length at which the bosonic three-body loss time scale becomes shorter than the experimental hold time, based on our variational model. The inset shows a typical TOF image of ^{87}Rb atoms in the loss-dominated regime, for low N_f. The cross indicates the associated experimental parameters ($V_0 = 11 E_r$, $a_{bf} = -480a_0$).

bosonic and fermionic Gaussian density profiles for given V_0 and occupation numbers. For all practically relevant boson numbers, we find that for sufficiently strong attractive a_{bf}, the on-site density collapses. The density increase in the vicinity of this collapse gives rise to an enhanced bosonic three-body loss rate $\dot{N}_3$ due to the $\dot{N}_3 \propto \sigma_b^{-6}$ scaling. For practical purposes, a site can be considered lost when $\dot{N}_3 \tau \gg 1$, where τ is the experimental hold time. Assuming a loss coefficient for collisions of three ^{87}Rb atoms in the range $K_3 = 4 \ldots 7 \times 10^{-30}$ cm^6/s [20], we find that lattice sites with four or more bosons will be lost on time scales faster than our hold time even in the absence of fermions. On the other hand, the observed ratio of lost ^{87}Rb to ^{40}K atoms between 3 and 4 suggests that three-body losses of two bosons together with one fermion do not play a significant role in our system. This observation is consistent with the measurements presented in [12]. Therefore, we focus our attention on sites occupied by three bosons and one fermion. The critical scattering length at which $\dot{N}_3 \tau = 1$ for bosonic three-body losses, derived from our variational model, shows good agreement with the experimentally observed onset of the loss-dominated regime, as can be seen in Fig. 2(c). We therefore conclude that for strong attraction, the dominant process is the loss of highly occupied sites enhanced by the interaction-induced density accumulation, commonly referred to as self-trapping [10,21]. The associated increase of the visibility could be thought of as the removal of strongly localized atoms on highly occupied sites from the system, and thus an enhancement of the boson mobility.

In order to investigate the persistence of bosonic superfluidity in the mixture, we extract the condensate fraction

from the recorded TOF images. This is done by fitting anisotropic two-dimensional bimodal Gaussians to all first-order diffraction features as well as the central peak after substraction of a broad Gaussian background from the image. The condensate fraction, which we define as the sum of the atom numbers in the narrow features at quasi-momentum zero and the eight first-order peaks, divided by the total atom number (see also Ref. [22]), is found to decay monotonically towards zero with increasing lattice depth for all values of a_{bf} at all fermion numbers.

The point in lattice depth at which the condensate fraction vanishes depends strongly on the interaction strength (Fig. 3). To quantify this point, we fit a linear decrease model to our data, thus obtaining the kink position for each scattering length (inset of Fig. 3). For medium to high N_f, the transition points lie almost on top of each other, both displaying a strong shift of up to $10 E_r$ towards shallower lattices for attractive interactions. In this regime, we expect the bosons to move on top of an essentially homogeneous fermion filling. The fermions then constitute an effective attractive potential for the bosons, which adds to the depth of the lattice potential. The shift can thus be understood in terms of an effective deepening of the lattice sites induced by the Bose-Fermi attraction, which modifies both the boson tunneling and interbosonic repulsion. As soon as the interspecies attraction overcomes the bosonic repulsion, the formation of a bosonic MI shell of filling two is energetically favored, resulting in even deeper effective
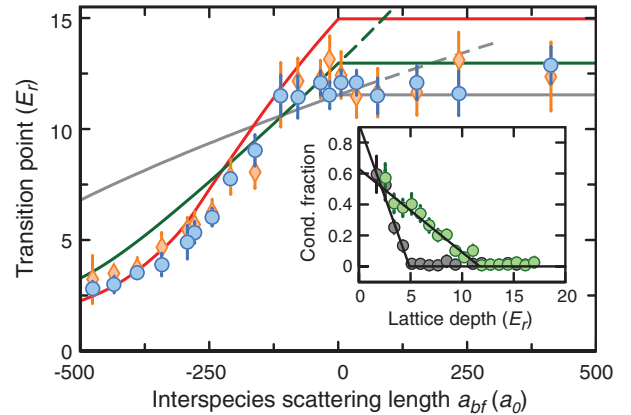

FIG. 3 (color).   Shift of MI transition point with interspecies interaction. The diamonds and circles represent experimental runs at medium and high fermion numbers, respectively. The error bars incorporate the fit uncertainty and the weighted average over typically two experimental runs. The lines indicate the theoretical MI transition point as estimated by the variational model for filling one (solid gray line), as well as exact diagonalization predictions for MI fillings of two (solid red) and one (solid green). For $a_{bf} > 0$, the solid lines correspond to a phase separation scenario, while the respective mixed phase predictions are depicted by dashed lines. The inset exemplarily shows the behavior of the condensate fraction at intermediate N_f, for $a_{bf} = -295a_0$ (black points) and $a_{bf} = 235a_0$ (green points), respectively.

potentials, thereby further enhancing the modification of the Hubbard parameters. The variational model (gray line in Fig. 3) clearly underestimates the self-trapping and thus yields smaller shifts than experimentally observed. A single-site exact diagonalization approach for the effective Hubbard parameters including the full orbital degrees of freedom [10] (solid red and green lines in Fig. 3) shows good agreement with the experimental data [23]. This supports that the shift of the transition point in the attractive regime can be explained by self-trapping. For repulsive interactions, a shift towards deeper lattices of comparable magnitude is predicted by the same model, assuming a homogeneous distribution of bosons and fermions throughout the lattice. The absence of a significant shift in this direction indicates that bosons and fermions do not occupy the same lattice sites in that regime. For low N_f, where the assumption of a homogeneous fermion filling is not valid, the decrease of the condensate fraction shows a more complex behavior which can not be captured by a linear slope, and the discussion of which is beyond the scope of our model.

In conclusion, we have explored the quantum phases of a mixture of bosonic ^{87}Rb and fermionic ^{40}K in a 3D optical lattice. By tuning the interspecies interaction and lattice depth, we have observed transparency of the fermions at $a_{bf} = 0$, and a symmetric decay of visibility in a small window around that point. The condensate fraction shows a behavior which we interpret as a shift of the bosonic MI transition towards shallower lattice depths with increasing interspecies attraction. We attribute this shift to a renormalization of the parameters of the effective Bose-Hubbard model by self-trapping, and find good quantitative agreement with an exact diagonalization calculation. We expect this effect to also play a major role in understanding the steep visibility decay for intermediate interspecies attraction away from the MI transition. Our results suggest that Feshbach-assisted lattice loading can be used to tailor the resulting lattice filling. Finally, the observed transparency is a promising starting point for experiments on tunable impurities [19,25,26].

*Present address: FOM Institute for Atomic and Molecular Physics (AMOLF), Kruislaan 407, 1098 SJ Amsterdam, The Netherlands

[1] A. Albus, F. Illuminati, and J. Eisert, Phys. Rev. A **68**, 023606 (2003).

[2] A. B. Kuklov and B. V. Svistunov, Phys. Rev. Lett. **90**, 100401 (2003).

[3] M. Lewenstein, L. Santos, M. A. Baranov, and H. Fehrmann, Phys. Rev. Lett. **92**, 050401 (2004).

[4] L. Mathey, D.-W. Wang, W. Hofstetter, M. D. Lukin, and E. Demler, Phys. Rev. Lett. **93**, 120404 (2004).

[5] M. Cramer, J. Eisert, and F. Illuminati, Phys. Rev. Lett. **93**, 190405 (2004).

[6] C. N. Varney, V. G. Rousseau, and R. T. Scalettar, Phys. Rev. A **77**, 041608(R) (2008).

[7] A. Zujev, A. Baldwin, R. Scalettar, V. Rousseau, P. Denteneer, and M. Rigol, Phys. Rev. A **78**, 033619 (2008).

[8] H. P. Büchler and G. Blatter, Phys. Rev. Lett. **91**, 130404 (2003).

[9] I. Titvinidze, M. Snoek, and W. Hofstetter, Phys. Rev. Lett. **100**, 100401 (2008).

[10] D.-S. Lühmann, K. Bongs, K. Sengstock, and D. Pfannkuche, Phys. Rev. Lett. **101**, 050402 (2008).

[11] M. Cramer, S. Ospelkaus, C. Ospelkaus, K. Bongs, K. Sengstock, and J. Eisert, Phys. Rev. Lett. **100**, 140409 (2008).

[12] K. Günter, T. Stöferle, H. Moritz, M. Köhl, and T. Esslinger, Phys. Rev. Lett. **96**, 180402 (2006).

[13] S. Ospelkaus, C. Ospelkaus, O. Wille, M. Succo, P. Ernst, K. Sengstock, and K. Bongs, Phys. Rev. Lett. **96**, 180403 (2006).

[14] J. Catani, L. DeSarlo, G. Barontini, F. Minardi, and M. Inguscio, Phys. Rev. A **77**, 011603(R) (2008).

[15] C. Klempt, T. Henninger, O. Topic, J. Will, W. Ertmer, E. Tiemann, and J. Arlt, Phys. Rev. A **76**, 020701(R) (2007).

[16] The harmonic trap is oblate, with a vertical symmetry axis. Effective horizontal and vertical confinement frequencies for lattice depth of 2 (17) E_r are (32, 113) Hz [(28, 112) Hz] for ^{87}Rb and (44, 194) Hz [(31, 191) Hz] for ^{40}K. For more details, see Th. Best *et al.* (to be published). At $a_{bf} = 0$, we expect a bosonic MI of filling one, possibly with a small core of filling two. Note that for $a_{bf} \ll 0$, the filling is dictated by the atom number ratio rather than the trap, and should approach two.

[17] F. Gerbier, A. Widera, S. Fölling, O. Mandel, T. Gericke, and I. Bloch, Phys. Rev. Lett. **95**, 050404 (2005).

[18] Phase separation in the lattice might be promoted by the slightly different trap shapes for the two species.

[19] A. Mering and M. Fleischhauer, Phys. Rev. A **77**, 023601 (2008).

[20] E. A. Burt, R. W. Ghrist, C. J. Myatt, M. J. Holland, E. A. Cornell, and C. E. Wieman, Phys. Rev. Lett. **79**, 337 (1997).

[21] M. Bruderer, W. Bao, and D. Jaksch, Europhys. Lett. **82**, 30004 (2008).

[22] I. B. Spielman, W. D. Phillips, and J. V. Porto, Phys. Rev. Lett. **100**, 120402 (2008).

[23] Assuming a critical ratio of $U/J = 29.3$ (49.8) for bosonic filling 1 (2), see [24].

[24] B. Capogrosso-Sansone, N. V. Prokof'ev, and B. V. Svistunov, Phys. Rev. B **75**, 134302 (2007).

[25] U. Gavish and Y. Castin, Phys. Rev. Lett. **95**, 020401 (2005).

[26] K. V. Krutitsky, M. Thorwart, R. Egger, and R. Graham, Phys. Rev. A **77**, 053609 (2008).